polymer papers

Diffraction measurements of crystalline morphology in a thermotropic random copolymer

D. J. Wilson, C. G. Vonk and A. H. Windle*
Department of Materials Science and Metallurgy, University of Cambridge, Pembroke Street, Cambridge CB2 3QZ, UK
(Received 2 March 1992)

The crystal structure and morphology has been examined in a series of 4-hydroxybenzoic acid (HBA) and 2-hydroxy-6-naphthoic acid (HNA) thermotropic random copolymers having different compositions and molecular weights. For rapidly cooled HBA-rich samples, the structure is pseudo-hexagonal, while for the more HNA-rich it is slightly distorted to orthorhombic, a phase designated O″. On annealing, the HBA-rich samples undergo a partial phase transformation to a denser orthorhombic phase with a greater distortion from the hexagonal than the O″. This new phase is designated O′. Annealing of the samples richer in HNA leads to a greater distortion of the O″ cell away from hexagonal, but no increase in density. Discrete small-angle diffraction maxima corresponding to a long period of ~300 Å appear only in those samples containing the denser O′ phase, with the implication that both pseudo-hexagonal and O″ crystals have densities very close to that of the non-crystalline nematic matrix. Anneals above 230°C lead to a marked increase in long period and there was some evidence of a specific doubling mechanism. Precise measurement of crystallinity gave values between 17.5% and 25.5%, the lower values being in the samples closer to the 1:1 composition and in those annealed.

(Keywords: liquid crystalline polymers; thermotropic random copolymers; wide-angle X-ray scattering; small-angle X-ray scattering; degree of crystallinity)

INTRODUCTION

This paper reports an investigation of the structure of a series of thermotropic liquid crystalline aromatic copolyesters based on 4-hydroxybenzoic acid (HBA) and 2-hydroxy-6-naphthoic acid (HNA). Polymers of this type are known to be partially crystalline, and crystallites have previously been detected by wide-angle X-ray scattering (WAXS)[1,2], scanning electron microscopy of etched surfaces[3] and transmission electron microscopy[4,5]. WAXS demonstrates the possibility of two crystal structures in the HBA–HNA copolymers. The unoriented mid-range composition materials crystallize as a metastable pseudo-hexagonal (PH) structure, which transforms on annealing to an orthorhombic phase[6–8]. More recently, the observation has been reported for thermally annealed, melt-spun fibres[9].

The present work is a diffraction study of a novel series of low molecular weight HBA–HNA analogues. The development of discrete small-angle X-ray scattering (SAXS) maxima on annealing has been correlated with distinct changes in the WAXS pattern for a range of molecular weights and chain compositions.

In addition, an absolute degree of crystallinity is determined in a rigorous manner, which, when combined with measurements of SAXS long periods, provides a means of estimating the crystal thickness. Furthermore, the observation of long period doubling in liquid crystalline polymers is unprecedented, illustrating an intriguing similarity in behaviour to the crystallization of some conventional polymers.

*To whom correspondence should be addressed

SAXS studies of synthetic polymers

One of the principal areas of application for SAXS has been the morphological investigation of synthetic polymers, since the periodicities which are encountered are invariably within the range of 10–1000 Å. The most thoroughly studied material in recent years has been melt-crystallized polyethylene[10–15]. Crystal thickening on annealing can be followed through the shift of the diffraction maxima to lower angles. Annealing also appears to sharpen the crystal profile leading to better defined high order maxima[14]. There is some evidence for the occurrence of an annealing mechanism which leads to a doubling of crystal thickness. Seen first for polyamides crystallized from solution[16], there have been subsequent reports, based on analysis of WAXS line profiles, of a similar effect in solution-crystallized polyethylene[17]. On the other hand, the evidence for the doubling of *long period* in melt crystallized polyethylene has been explained by one of us[15] in terms of a mechanism akin to Ostwald ripening. This process occurs at annealing temperatures where the critical nucleus size approaches the crystal size and there is competition between crystal melting and crystal growth, the melting of a crystal thus enhancing the growth prospects of its two immediate neighbours.

SAXS has since been employed on a number of occasions to explore the morphological features of liquid crystalline polymers. The main feature in the diffraction patterns of the lyotropic polymer, Kevlar™, is a continuously decreasing streak along the equator. This is generally attributed to elongated voids, although recent research has shown that it may also be derived from

0032-3861/93/020227-11

the crystals in the fibre[18]. Baltá Calleja *et al.*[19] investigated the influence of composition on the molecular structure of the semiflexible main-chain thermotropic copolymer composed of poly(ethylene terephthalate) and 4-acetoxybenzoic acid. They found that the long periods of samples which had been annealed for 4 h at temperatures close to the melting point did not appear to depend markedly upon composition.

The earliest observation of SAXS from the rigid main-chain copoly(HBA–HNA)[20] did not reveal any discrete diffraction maxima, and was largely an attempt to determine the appropriate Friedelian structural classification for the material. Only very recently has SAXS been used to confirm the actual presence of crystallites in HBA–HNA[21]. In this instance, small-angle meridional diffraction was observed from moderately annealed fibres, when it indicated the development of scattering entities with an average separation distance of ~200–300 Å.

Previous estimates for the crystallinity of copoly(HBA–HNA)

Blundell[22] estimated a degree of crystallinity of 21% for the high molecular weight copolymer containing 60 mol% HNA. Flakes of the polymer were loaded into capillary tubes, heated to fuse the material and melt quenched. Scans were then obtained in transmission, and the percentage crystallinity was obtained by subtracting an estimated amount of incoherent scattering from the diffraction pattern, and then determining the distribution of scattering intensity between the crystalline and amorphous parts of the diffraction pattern. The melt profile was scaled down and fitted under the crystalline peaks to represent the amorphous phase.

Butzbach *et al.*[23] obtained a degree of crystallinity for B-N 58:42* of 30% for an unannealed sample and ~60% for a well annealed sample, although they do not describe the technique which was employed. It appears that the X-ray diagram of the melt phase was used to represent the amorphous content of the polymer, but there is no indication of the crucial correction for incoherent scattering. In this case, isotropic samples had been prepared by pressing films at a temperature of 300°C.

Hanna *et al.*[21] determined the crystallinity of a low molecular weight sample of B-N 3:1 which had been spread onto a silicon wafer, melt quenched, annealed, requenched and analysed. A value of 19% was obtained (after annealing at 200°C) by the conventional method of baseline estimation and area measurement described above. Spontak and Windle[5] estimated the crystallinity in the same material using electron microscopy. Based upon a crystallite separation distance of 75 nm, they obtained a value of 13% for a sample which had been sheared and annealed at 200°C. Furthermore, it was noted that crystallites may have been lost through damage during irradiation, and that this result was therefore likely to be an underestimate. They were unable to quantify the crystallinity of the corresponding high molecular weight copolymer, but proposed that it was probably as high as 15% and certainly much less than 50%. It is interesting to note that the crystallinity of poly(HBA) has previously been estimated to be above 75%[24] and that of poly(HNA) to be close to 50%[25].

As far as X-ray methods for determining the degree of crystallinity are concerned, the approach described by Ruland[26] is generally considered to have the best theoretical foundation and is most universal in its application. It is the approach used here.

*Copolymers of HBA and HNA are referred to as B-N followed by the ratio of the units, for example, B-N 58:42 represents a random copolymer consisting of 58% units derived from HBA and 42% from HNA

MATERIALS

The samples are a series of random copolyesters of 4-hydroxybenzoate (HBA) and 2-hydroxy-6-naphthoate (HNA) units, of a range of compositions and molecular weights:

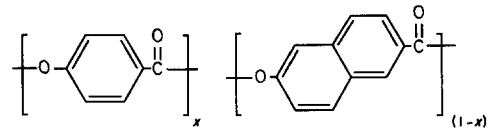

The samples were supplied by the Hoechst-Celanese Corporation (Summit, NJ, USA), and their details are recorded in *Table 1*. They were melt synthesized from appropriate ratios of the acetylated monomers, the molecular weight being controlled by terminating the reaction through the metered addition of terephthalic acid. No other additives or catalysts were used.

EXPERIMENTAL

Fibres were drawn on a hot stage at ~50°C above the melting point of the polymer, and then quenched to room temperature. Isothermal annealing treatments were carried out on unconstrained samples in an air-circulation oven prior to quenching onto a brass block at room temperature. The anneals were all for 6 h at temperatures ranging from 70–80°C below the melting point to as close to the sample melting point as was practicable.

Wide-angle X-ray photographic patterns were obtained from single fibres using a transmission flat-film camera with crystal-monochromatized CuKα radiation, the sample–film distance being 3.75 cm. The films were measured using a travelling microscope. The powder diffractometry was carried out in the Bragg–Brentano arrangement using a Siemens D500 TT instrument, employing nickel-filtered CuKα radiation.

SAXS measurements were made using a Kratky camera with nickel-filtered CuKα radiation, the fibre axis being perpendicular to the slit collimation system. The quality of molecular orientation was sufficiently high to enable the intensity distribution as projected on the fibre

Table 1 Copolyesters of HBA–HNA used in this study with composition, melting point and molecular weight

Sample number	HBA–HNA ratio	Melting point (°C)	M_w[a]
1	4:1	306	6100
2	3:1	271	4600
3	3:1	272	5000
4	3:1	274	8600
5	3:1	288	14 400
6	2:1	229	5200
7	1:1	228	5800
8	1:3	274	6200

[a] M_w is the weight-average molecular weight, based on viscosity measurements (Hoechst-Celanese Corporation)

Table 2 Diffraction data obtained at room temperature from the sample series for a range of annealing temperatures (6 h at temperature, T_a)

Sample number	HBA–HNA ratio	Mean molecular length (Å) (M_w)		Increasing anneal temperatures, T_a (6 h anneals) →							
1	4:1	315	T_a	U[a]	215	233.5	251	260.5	269	278	288	*
		(6100)	W[b]	O′+II	O′+II	O′+II	O′+II	O′+II	O′+II	O′+II	O′+II	*
			S[c]	Z	320w	390	410	430	470	495	530	*
			X[d]	22.5	*	17	*	*	25.5	*	*	*
2	3:1	240	T_a	U	196.5	215	233.5	251	260.5	265	269	278
		(4600)	W	PH	PH	O′	O′	O′+N	O′+N	O′+N	O′+N	O′+N
			S	–	280w	300	315+510	530	580	~640sh	~680sh	~735sh
			X	22.5	*	21	*	20.5	*	*	17	*
3	3:1	260	T_a	U	196.5	215	233.5	251	260.5	265	269	*
		(5000)	W	PH	O′	O′	O′	O′+N	O′+N	O′+N	O′+N	*
			S	–	280	290	310+585w	310w+590	600	640	~660	*
			X	22	*	21	*	20	*	*	17	*
4	3:1	440	T_a	U	196.5	215	233.5	251	260.5	269	278	288
		(8600)	W	PH	PH	PH	O′+II	O′+II	O′+N_w+II	O′+N_w+II	O′+N+II	O′+N+II
			S	–	–	330	400	465	500	~560sh	~630sh	~700sh
			X	22	*	*	*	19.5	*	*	17.5	*
5	3:1	740	T_a	U	196.5	215	233.5	251	269	278	288	*
		(14400)	W	PH	PH	PH	PH	O′+II	O′+II	O′+II	O′+II	*
			S	–	–	Z	~315	460	540	~610sh	~680sh	*
			X	20.5	*	*	*	17.5	*	*	*	*
6	2:1	270	T_a	U	140.5	159	177	187	196.5	206	215	233.5
		(5200)	W	PH	PH	PH	PH	O″+O′	O″+O′	O″+O′	O″+O′+N	O″+O′+N
			S	–	–	–	–	280w	300w	320w	~335w	Z
			X	22	*	*	*	*	21	*	*	*
7	1:1	290	T_a	U	159	177	196.5	215	233.5	*	*	*
		(5800)	W	PH	PH	O″	O″	O″	O″	*	*	*
			S	–	–	–	–	–	–	*	*	*
			X	18	*	*	*	18	*	*	*	*
8	1:3	310	T_a	U	196.5	215	233.5	251	260.5	269	278	*
		(6200)	W	O″	O″	O″	O″	O″	O″	O″	O″	*
			S	–	–	–	–	–	–	–	–	*
			X	21	*	*	*	19	*	*	*	*

[a]U indicates that the sample was examined as-drawn, without any subsequent annealing
[b]The rows marked W refer to the WAXS patterns, PH indicating the pseudo-hexagonal phase and O′ and O″ orthorhombic phases in which the 1 1 0 and 2 0 0 reflections are clearly separated. The notations II and N refer to the presence of a second phase [related to that seen in poly(HBA)] and additional reflections, respectively, and are discussed in the text
[c]The rows marked S refer to the SAXS patterns. Where a discrete maximum was apparent, the long spacing is recorded in Å. Z implies strong scattering without discrete maxima, while the suffixes w or sh imply that the peak is either weak or appears as a small shoulder on a steeply sloping background. – indicates that no significant small-angle scattering was detected
[d]The rows marked X give the crystallinity of the samples where this has been measured by powder diffractometry
In general, * indicates that no measurement was made

axis to be used directly without desmearing. The small-angle scattering was recorded on Reflex 25 double emulsion film manufactured by CEA, and quantified by scanning on a Joyce-Loebl double-beam microdensitometer. Optical densities were converted to X-ray intensities according to Vonk and Pipjers[27].

The majority of the experimental results are collated and summarized in *Table 2* which includes phase identification based on WAXS fibre patterns, long periods from the SAXS data, and crystallinities from powder diffractometry. The data are presented for samples of different composition, molecular weight and heat treatment.

WIDE-ANGLE DIFFRACTION STUDIES

Indexing the wide-angle fibre patterns

The wide-angle diffraction data confirm the occurrence of the so-called PH phase in all as-drawn samples of B-N[28]. This phase is characterized by a single, very intense equatorial reflection (which indexes as 1 1 0 with respect to an orthorhombic cell) and two clearly

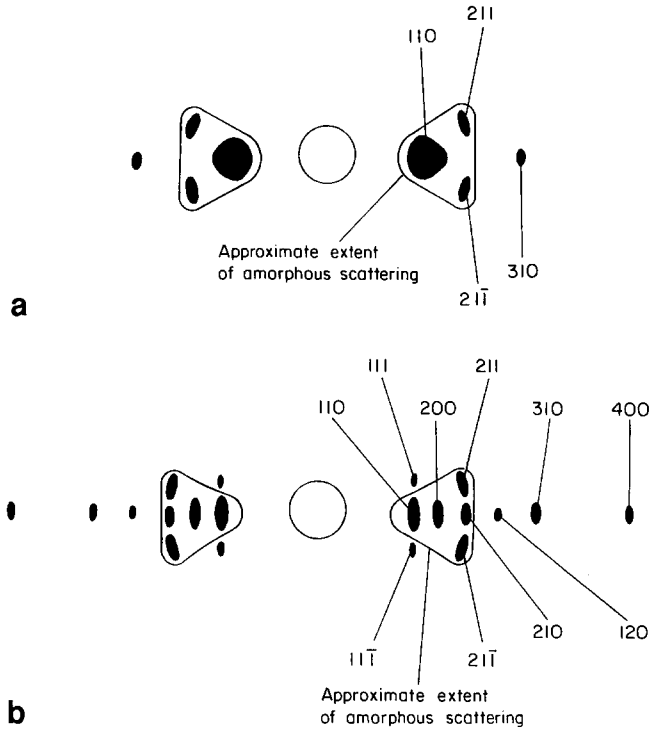

Figure 1 Positions of reflections on and near the equator as observed on flat-film exposures: (a) PH phase; (b) O′ phase. The fibre axis is vertical. Note that the observation of either (a) or (b) is dependent upon composition, molecular weight and heat treatment, as indicated in *Table 2*

discernible reflections as shown schematically in *Figure 1a*. In addition, there is a diffuse region of diffracted intensity centred on the equator which is associated with the non-crystalline phase. Furthermore, three, and in the case of the B-N 1:3 sample, four, meridional reflections are visible. Their positions are in accordance with the presence of HBA and HNA units, distributed in random order along the chains, as discussed by several authors[1,29,30].

The criterion used for indexing a phase as PH rather than orthorhombic is that there is no discernible splitting of the 1 1 0 peaks into 1 1 0 and 2 0 0 maxima. It is possible therefore that an orthorhombic phase in which a/b is very close to $\sqrt{3}$ will be classified as PH owing to the impossibility of resolving the 1 1 0 and 2 0 0 peaks which are close and overlapping. As can be seen from the powder diffractometer scan in *Figure 2*, the half-widths of the 1 1 0 and 2 1 1 maxima are between 1°2θ and 3°2θ.

On the basis of very close or essentially overlapping 1 1 0 and 2 0 0 peaks in the HBA-rich polymers, and the clearly resolvable pair in polymers containing 33% HNA or more (samples 6–8, *Figure 3*), the significant off-equatorial reflections index as 2 1 1 and 2 1 $\bar{1}$. The equatorial maximum at the higher angle in *Figure 1a* could, at first sight, be either 310, 120 or 020. In choosing between these options, we carefully measured and analysed the positions of the peaks on 17 flat-film photographs in which separation of the 1 1 0 and 2 0 0 could be resolved. Of the three choices, the 3 1 0 option showed the best correlation, and in the 3:1 samples was also consistent with the fact that the 1 1 0 and 2 0 0 reflections were not separately resolvable. The indices shown in *Figure 1a* are based on this indexing scheme. It should also be noted that the presence of a 2 1 1 reflection is not consistent with a primitive hexagonal lattice cell, which corresponds to a C-centred orthorhombic cell. The occurrence of this reflection is sufficient to justify the choice of a P or I orthorhombic cell, which is known here as PH when the 1 1 0 and 2 0 0 peaks are coincident or at least too close to be distinguished, implying that $a \approx \sqrt{3}b$.

Table 2 shows that for the samples with B-N ratios of >1:1, an *orthorhombic* phase, designated O′, appears in samples annealed at temperatures of 200°C and above (with the exception of B-N 4:1 which is orthorhombic on quenching). The reflections on and near to the equator index as orthorhombic in accord with the proposals originally cited for poly(HBA)[31], and are illustrated in *Figure 1b*. The first and most noticeable feature of the orthorhombic phase is the occurrence of the relatively strong 2 0 0 reflections at a larger angle than the 1 1 0, which itself is not markedly shifted with respect to the position of the 1 1 0 reflection of the PH phase. Another intriguing aspect is the occurrence, on annealing, of two apparently distinct orthorhombic phases in 2:1 samples. We distinguish them here by the designations O′ and O″. In O″, the 2 0 0 peak is very close to the 1 1 0, while in O′ it is separated from it by ~3.5°2θ. A further distinction is that the 'close' 2 0 0 peak in O″ moves to significantly higher angles on annealing, while the position of that in O′ changes to a lesser extent. Furthermore,

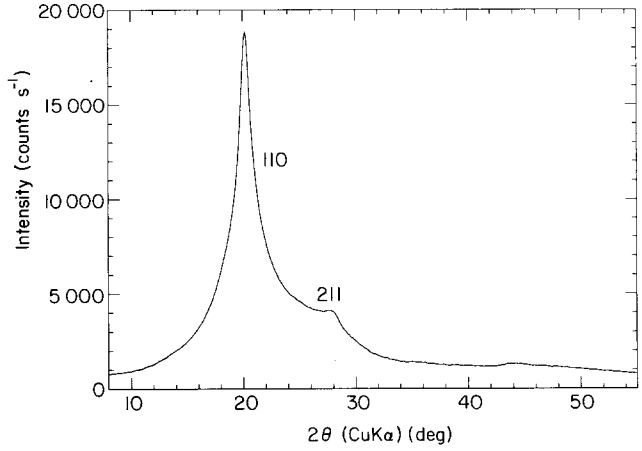

Figure 2 Powder diffraction curve for an unannealed (as-quenched) specimen of B-N 3:1 (sample 3)

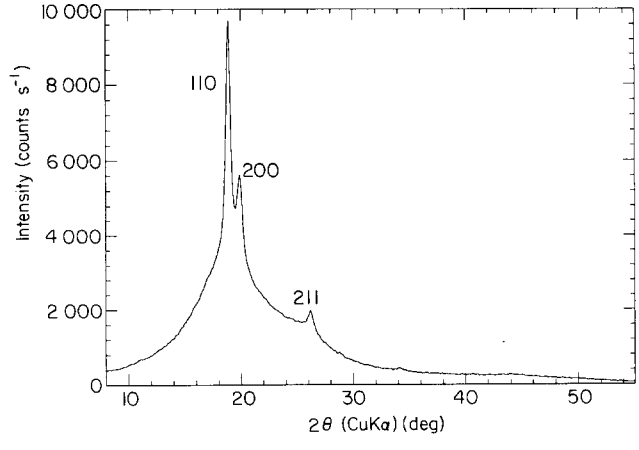

Figure 3 Powder diffraction curve of sample 8 (B-N 1:3) held at 220°C showing the resolution of 1 1 0 and 2 0 0 reflections in the O″ phase

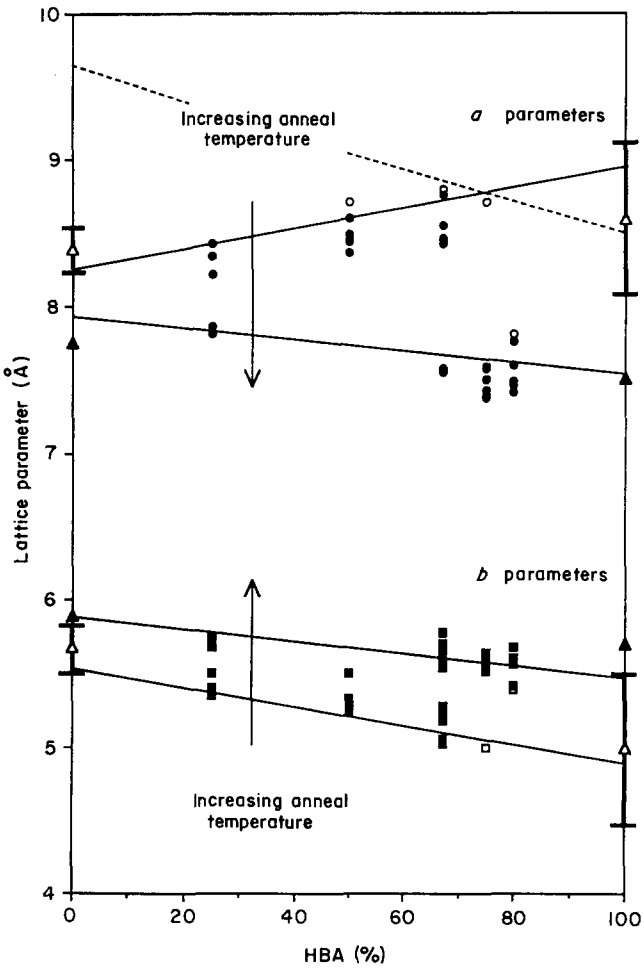

Figure 4 a and b lattice parameters for different heat treatments as a function of composition of the HBA/HNA copolymers (M_w = 5000–6200). The top and bottom lines are drawn through the empty symbols representing the unannealed polymers. The lines are least squares fits, and it should be noted that some of the open symbols are obscured amongst the solid ones. The broken line represents the value of the a parameter which is $\sqrt{3}$ times that of b, so that given the b values, the a parameters would lie on this line if the cell was exactly hexagonal. The two central lines are drawn through the (solid) points corresponding to the highest temperature anneals of the copolymers recorded in *Table 3* and the previously measured data for the homopolymers[24,25]: (○) a (unannealed); (□) b (unannealed); (●) a (annealed); (■) b (annealed); (▲) homopolymer; (△) homopolymer (extrapolated from high-temperature pseudo hexagonal phases)

compositions which are more HBA-rich than 2:1 show only the O′ phase, while those which are more HNA-rich possess only the O″ structure. As the 1 1 0 maxima of the orthorhombic phases are at the same scattering angle as the PH 1 1 0 reflection, the identification of an orthorhombic component cannot be taken as implying the absence of PH. Indeed, the relative magnitudes of the 1 1 0 and 2 0 0 maxima observed in both HBA and HNA homopolymers suggest that the PH phase may always be present in the HBA-rich copolymers, whether or not the O′ phase is present.

Influence of composition and annealing on the unit cell

Figure 4 shows the variation in the a and b parameters of the unit cell as a function of composition and annealing. The open circles or squares correspond to the lattice parameters of the random copolymer fibres as-drawn (except for the two homopolymers – see below), while the sequences of solid points plot the lattice parameters of fibres annealed for 6 h at the increasing temperatures indicated in *Table 3*.

Lattice parameters of homopolymers. Both poly(HBA) and poly(HNA) homopolymers show orthorhombic structures at room temperature. These have been reported by a number of authors and the data used here are those from references 2, 24 and 25. The a and b parameters for 0 and 100% HBA are plotted on the vertical axes of *Figure 4* as solid triangles. Both homopolymers show PH phases at elevated temperatures, above 350°C for poly(HBA) and between 400°C and 445°C for poly(HNA). The values of a and b corresponding to the PH structures of the homopolymers, and plotted as open triangles, were obtained by extrapolating to room temperature the plot of lattice parameter against temperature[24] in the high temperature region of PH stability. The uncertainty associated with this procedure is accounted for by the error bars in *Figure 4*. It is interesting to note how similar are the a–b cross-sectional areas of the two orthorhombic homopolymer cells (solid triangles), that of poly(HNA) being only 6.5% larger in area than that of poly(HBA).

HBA-rich compositions (2:1, 3:1 and 4:1). The 2:1 and 3:1 compositions show a PH phase in the as-drawn fibres in that the 1 1 0 and 2 0 0 peaks of an orthorhombic cell are inseparable, if not coincident. This observation is reflected in *Figure 4* in that the a parameters of these compositions lie close to the sloping broken line which is the line through the plots of the b parameters multiplied by $\sqrt{3}$. It should be noted that annealing induces the O′ structure in which the a and b parameters have values very close to those predictable from the homopolymer values on a pro rata basis. It is thus clear that packing between the chains in the annealed random copolymer crystals is every bit as efficient as in the homopolymers. The 4:1 sample is orthorhombic on quenching, and annealing has little effect upon the lattice parameters.

Two additional reflections are apparent in the otherwise orthorhombic diffraction patterns of annealed 4:1 and the two highest molecular weight 3:1 samples (4 and 5). They are thought to indicate the presence of a small amount of material which is the analogue of phase II poly(HBA)[24,31], and are denoted by II in *Table 2*. They occur at 15.9°2θ and between 22.4°2θ and 24°2θ, respectively, the latter peak position increasing in angle as the anneal temperature is raised or the percentage of HBA increased. The proportion of phase II present in the homopolymer of HBA has previously been shown to be dependent upon the preparation conditions[32].

One other type of observation should be recorded although it is not understood. Annealing the lower molecular weight polymers of composition B-N 2:1 and 3:1 at temperatures approaching the melting point, led to some of the layer line reflections of the orthorhombic pattern appearing to split into doublets displaced in the fibre axis direction. The degree of splitting appeared to vary between reflections of different indices. There was, however, no splitting of the meridional maxima. The presence of these reflections, where they were observed, are noted in *Table 2* by the letter N.

Compositions 1:1 and 1:3. As with the 4:1 polymer, these compositions show an orthorhombic phase in the as-drawn fibres. However, the phase is O″ rather than

Table 3 Lattice parameters a and b obtained from flat-film photographs along with the respective cross-sectional basal areas of the unit cells for different samples and different annealing treatments[a]

Sample number	HBA–HNA ratio		Increasing anneal temperatures, T_a (6 h anneals)						
1	4:1	T_a	U[b]	215	233.5	251	260.5	269	278	*[c]
		a	7.81/8.89	7.77	7.61	7.49	7.49	7.47	7.42	*
		b	5.39/5.13	5.42	5.57	5.60	5.60	5.63	5.59	*
		$a \times b$	42.1/45.6	42.1	42.4	41.9	41.9	42.1	41.5	*
3	3:1	T_a	U	196.5	215	233.5	251	260.5	269	*
		a	8.71	7.59	7.58	7.51	7.43	7.38	7.39	*
		b	5.00	5.59	5.64	5.52	5.61	5.58	5.62	*
		$a \times b$	43.6	42.4	42.8	41.5	41.7	41.2	41.5	*
6	2:1	T_a	U	140.5	159	177	187	196.5	206	215
		a	8.80	8.76	8.67	8.56	8.46/7.56	8.43/7.56	8.47/7.56	8.46/7.58
		b	5.04	5.03	5.06	5.20	5.18/5.54	5.24/5.65	5.28/5.59	5.28/5.70
		$a \times b$	44.4	44.1	43.9	44.5	43.8/41.9	44.2/42.7	44.7/42.3	44.7/43.2
7	1:1	T_a	U	159	177	196.5	215	233.5	*	*
		a	8.71	8.61	8.50	8.45	8.37	8.46	*	*
		b	5.25	5.26	5.30	5.33	5.41	5.51	*	*
		$a \times b$	45.7	45.3	45.1	45.0	45.3	46.6	*	*
8	1:3	T_a	U	196.5	215	233.5	251	260.5	269	*
		a	8.43	8.43	8.35	8.22	8.06	7.97	7.96	*
		b	5.36	5.36	5.41	5.50	5.60	5.64	5.68	*
		$a \times b$	45.2	45.2	45.2	45.2	45.1	45.0	45.2	*

[a]Agreement with diffractometer data is generally better than 1.25%. Note that sample 1 (B-N 4:1) is O′ at all temperatures, and the lattice parameters of $a = 8.89$ and $b = 5.13$ Å at room temperature for the PH phase have been calculated from the position of the 1 1 0 reflection, and are included for comparison in the format O′/PH for the unannealed 4:1 copolymer. In sample 6 (B-N 2:1) where the O′ and O″ phases occur together above 187°C, the lattice parameters and base areas are given in the format O″/O′. The homopolymer parameters at room temperature are: HBA, $a = 7.52$, $b = 5.70$; HNA, $a = 7.75$, $b = 5.89$ Å. The extrapolation from high-temperature PH phases gave: HBA, $a = 8.60$, $b = 5.00$; HNA, $a = 8.40$, $b = 5.68$ Å

[b,c]As defined in *Table 2*

O′ as discussed above. The 1 1 0 and 2 0 0 peaks form a clear doublet in the as-drawn 1:3 polymer, and can be seen as overlapping components in the 1:1 material, while annealing causes the unit cell parameters to drift gradually towards the 'equilibrium' line corresponding to the parameters seen in the HBA-rich samples and the homopolymers. In the case of the 1:3 polymer, the line is almost reached, whereas annealing has a much more limited effect on the 1:1 polymer. The reason for this reduced response in the case of the 1:1 material may well be associated with the fact that its melting point is significantly lower than for either 1:3 or 3:1 (228°C compared with 274 and 272°C, respectively).

Comparison of the annealing behaviour in HBA-rich and HNA-rich samples. The difference in annealing behaviour between HBA-rich and HNA-rich samples is worthy of more detailed attention. The cause is seen to be that the HBA-rich polymers start their annealing from a structure in which the unit cell has hexagonal symmetry, while in the case of the HNA-rich samples this state is never achieved; indeed the transition at 400°C on heating the homopolymer is from an orthorhombic structure to one which, although much closer to PH, always remains orthorhombic as the O″ phase. Now, if a structure transforms from hexagonal to orthorhombic (O′) it will be subject to transformation twinning (also known as multiple twinning). The process involves nearby cells distorting towards orthorhombic along different axes, and thus leads to significant internal strains. For this reason it will be more favourable for the new phase to grow by the process of nucleation and growth, so that the orthorhombic cells will all be similarly oriented on the new lattice, strains minimized and the equilibrium structure obtained. As the HNA-rich material never achieves hexagonal symmetry, the direction of distortion will always be defined and transformation will take place uniformly and gradually through the crystalline regions, only being limited by strains associated with the different densities of the crystalline and liquid crystalline phase[8]. Indeed, such an explanation would be consistent with the observation that the 2 0 0 of the O′ phase, in which transformation twinning is possible, is always broader than the 2 0 0 of O″.

Meridional reflections. The positions of the aperiodic meridional maxima appear to be unaffected by the PH to orthorhombic phase transformation, and are in good agreement with those cited by Chivers *et al.*[30]. In heavily exposed films, layer lines with $l = \pm 3$ and ± 5 can be seen, although they contain no meridional reflections.

Change in basal area of cell on annealing. Table 3 shows clearly that the tendency towards lattice parameters equivalent to the pro rata O′ phase on annealing gives rise to an increase in b and a decrease in a. These effects do not, however, exactly balance, and it is clear that in the HBA-rich 4:1 and 3:1 samples, the basal area of the

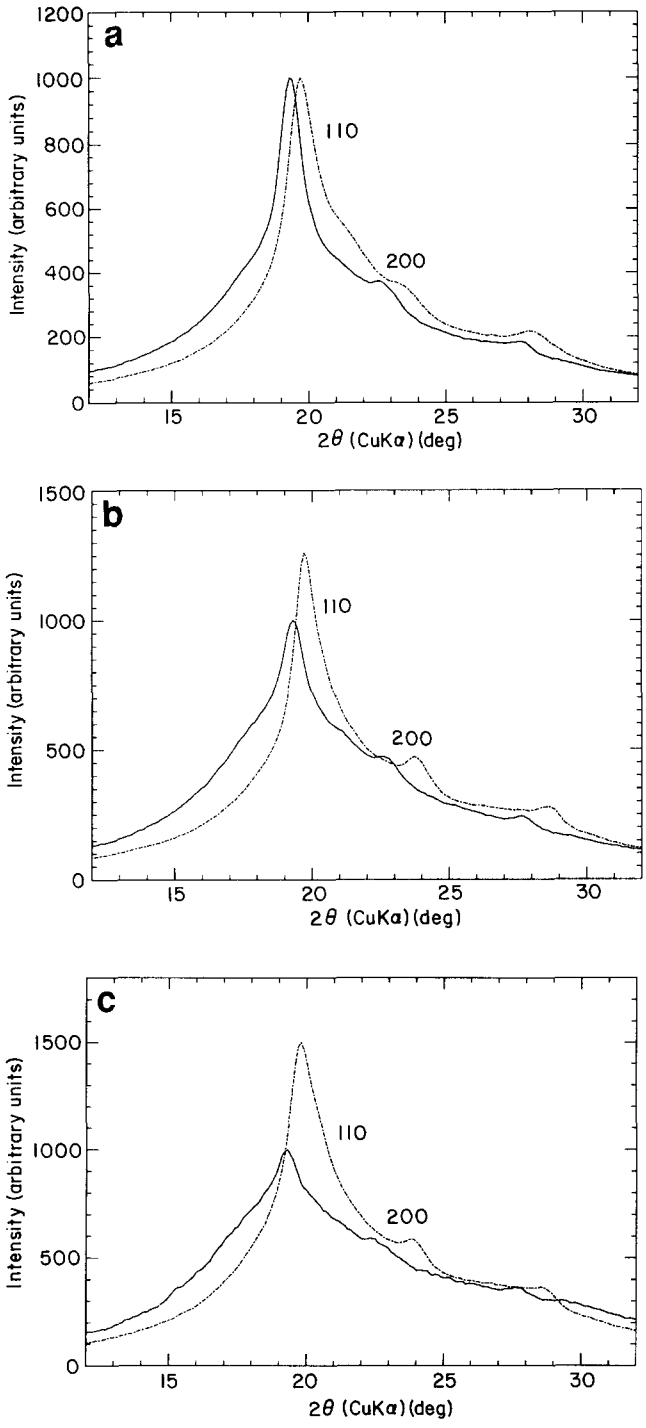

Figure 5 A series of six diffraction curves illustrating the effect of annealing temperature on O′ structure formation before (—) and after (—·) quenching sample 3 (B-N 3:1). The diffractometer data for the unannealed polymer were shown in *Figure 2*. Annealing temperature: (a) 215°C; (b) 251°C; (c) 269°C

cell is markedly less in the O′ phase than it is in the PH phase. Annealing the 1:1 and 1:3 samples produces a very distinct change in the a/b ratio (e.g. from 1.57 to 1.40 for 1:3) but no systematic change in basal area.

Influence of molecular weight on crystal structure

Table 2 shows, *inter alia*, data from samples of the molecular weight series which were all of composition 3:1. The most significant observation is that the transformation from PH to O′ required, for the fixed anneal period of 6 h, higher anneal temperatures for the higher molecular weight. The lowest temperature anneals necessary for the transformation were 196, 233 and 251°C, respectively, for the molecular weights 5000, 8600 and 14400. The implication of this observation is that the rate of transformation is controlled by some diffusive process which depends on the chain length. Whether this effect is associated with the relief of interfacial strains, or the enhancement of sequence matching, or both, remains to be demonstrated.

Crystal structure at the anneal temperature

In the comparatively low molecular weight materials studied, there is evidence that the O′ phase actually appears at the annealing temperature, and is not simply the result of the quenching process. *Figures 5a–c* show, for sample 3 (B-N 3:1), pairs of powder diffractometer scans. In each case the continuous trace was obtained actually at the anneal temperature, while the broken one was from the same sample after quenching to room temperature. The peak shifts are associated with thermal contractions, while the loss of crystallinity at the two higher temperatures is also very apparent. This behaviour is in contrast to that observed for high molecular weight material of the type marketed commercially as Vectra, where the O′ phase is only observed when the sample is cooled back to room temperature after the anneal[33].

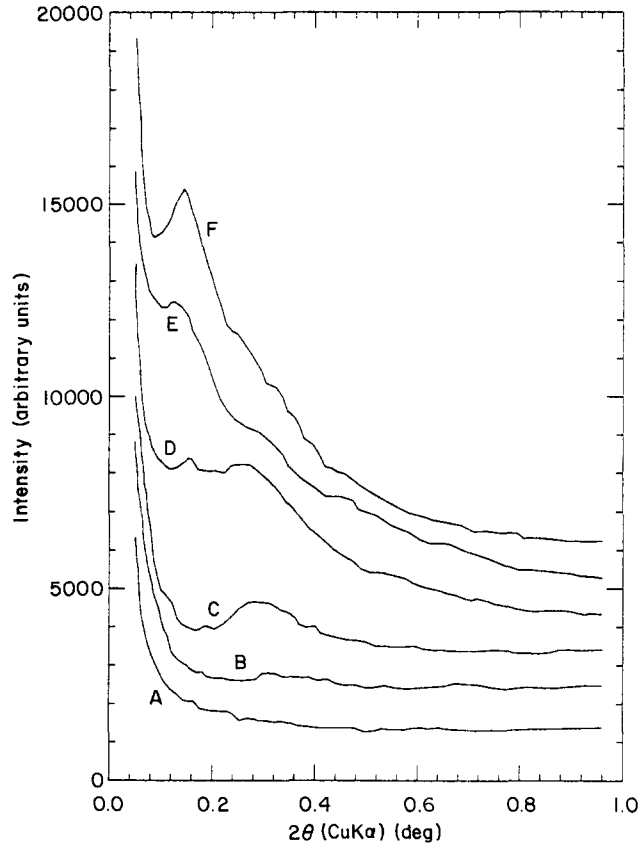

Figure 6 Meridional SAXS curves as obtained for sample 2 (B-N 3:1) after different annealing treatments. Trace A is for an unannealed specimen. Traces B–F are for samples annealed for 6 h at 196.5, 215, 233.5, 251 and 260.5°C, respectively. The increase in intensity at low angles represents the overspill from the primary beam. For clarity, subsequent curves have been displaced in the vertical direction. The observed long periods are as follows (trace number/small-angle maxima): A/no discrete maxima; B/280 Å; C/290 Å; D/310 + 585 Å; E/310 + 590 Å; F/600 Å

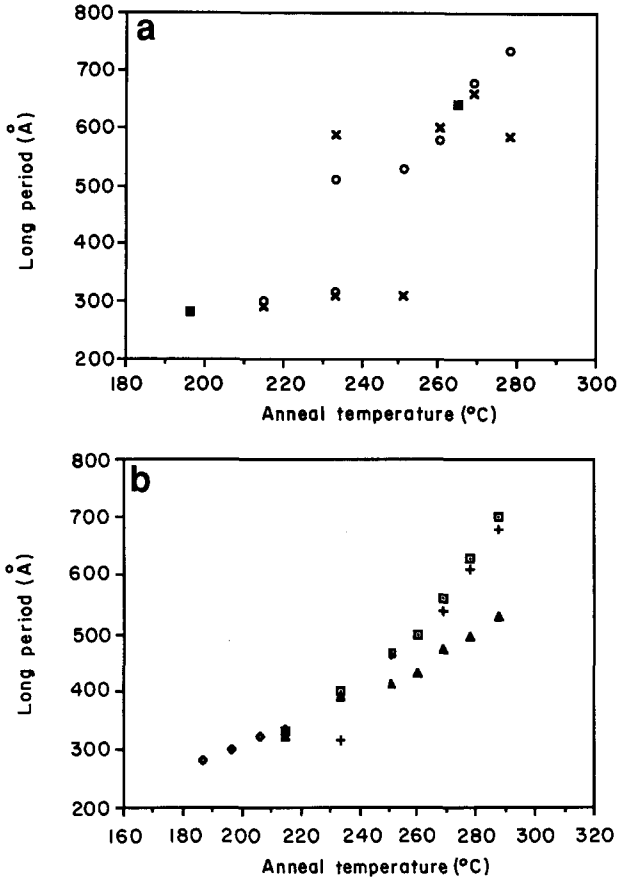

Figure 7 (a) Long periods *versus* anneal temperatures for the two lowest molecular weight samples of B-N 3:1. (b) Long periods *versus* anneal temperatures for all the samples which show continuous thickening. HBA–HNA ratio/M_w/sample number: (○) 3:1/4600/2; (×) 3:1/5000/3; (▲) 4:1/6100/1; (⊡) 3:1/8600/4; (+) 3:1/14400/5; (◇) 2:1/5200/6

SMALL-ANGLE X-RAY SCATTERING

The SAXS data, covering the range 10–1000 Å, are briefly summarized in *Table 2*, where they are classified under the general headings of discrete small-angle maxima, strong diffuse scattering and weak diffuse scattering.

Effect of annealing

Discrete small-angle maxima appear in annealed polymers with B-N ratios of $\geqslant$2:1. Within the margins of the observations, the appearance of the peak in the small-angle scattering corresponds to the formation of O′ phase. It is noteworthy that in nearly all these samples the first small-angle scattering to appear on annealing corresponds to a long period of ~300 Å, irrespective of the B-N ratio or the molecular weight. On further annealing, the scattering intensifies and is displaced to smaller angles as the long period increases. In the lower molecular weight samples with B-N 3:1 the increase occurs discontinuously: a new peak at about half the angle (twice the spacing) of the original peak develops and grows at the expense of the first. This process is illustrated in *Figure 6*, which shows the scattering curves obtained from sample 2 (B-N 3:1, molecular weight 4600) after different annealing treatments, while the long period is plotted against annealing temperature for both low molecular weight samples of 3:1 composition in *Figure 7a*. In other samples, higher molecular weight versions of 3:1 and the two other compositions for which the effect was observed, the shift of the maximum with increasing anneal temperature occurs in a more continuous manner as shown in *Figure 7b*. The underlying impression given by these data is that the long period and anneal temperature follow a relationship which is predominantly independent of molecular weight and of composition and thus melting point. It is also apparent that, for the B-N 3:1 sample at least, the temperature at which the small-angle scattering first appears increases linearly with the logarithm of the molecular weight (*Figure 8*).

It must be emphasized that the absence of discrete small-angle maxima does not imply the absence of crystallites which are always observable microscopically whatever the thermal protocol, composition or molecular weight[5,34,35].

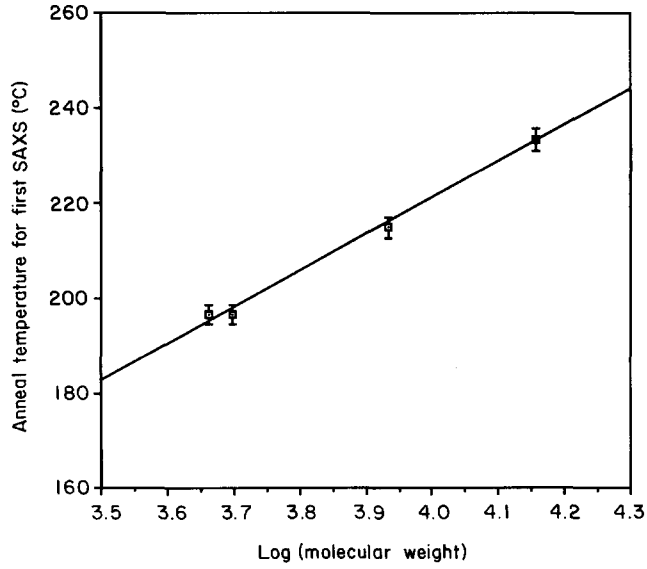

Figure 8 Dependence of anneal temperature for first observation of discrete SAXS on molecular weight for the B-N 3:1 copolymers. An anneal time of 6 h was employed, at temperatures ranging from 196.5 (M_w = 4600 and 5000) to 233.5°C (M_w = 14400)

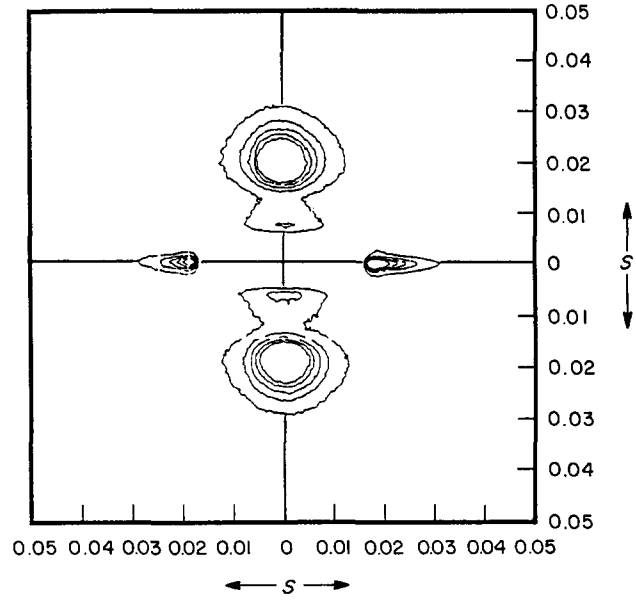

Figure 9 SAXS pattern of sample 3 (B-N 3:1), annealed at 215°C, as observed with a two-dimensional detector at the SERC facility in Daresbury. The fibre direction is vertical. The contours are at relative levels of 1, 2, 3, 4 and 5. Higher levels were omitted in order to give a clearer representation [$S = (4\pi/\lambda)\sin\theta$]

Two-dimensional scattering pattern

As mentioned before, the intensity curves obtained in the slit collimation SAXS experiments are in effect the projection onto the meridian of the intensity that would have been obtained with pin-hole collimation. In order to gain information regarding the lateral extension of the maxima in the fibre patterns, a pin-hole collimated pattern was obtained using synchrotron radiation from sample 3 (B-N 3:1) which had been annealed at 215°C. It is shown in *Figure 9*. Well-developed peaks on the meridian with a Bragg spacing of 300 Å are apparent, as are 'fibre streaks' on the equator. The diffraction is thus consistent with the occurrence of microfibrils within which crystalline and amorphous regions alternate along the fibre axis with a long period in the 300 Å range. From the width of the meridional maxima in the direction normal to this axis, one may conclude that the lateral extent of the order is at least 500 Å.

MEASUREMENT OF CRYSTALLINITY

Crystallinity was measured on macroscopically isotropic samples which were obtained by heating flakes of the starting material, quenching them to room temperature, and then annealing them for 6 h at the indicated temperatures before requenching. Scanning electron micrographs of fracture surfaces of such samples show them, on a microscopic level, to consist of fibrillar or 'lath-like' material[36]. It is therefore assumed that the results obtained on these samples would also relate to the fibres examined in the present study.

The scattering curves were recorded for scattering angles of 4–90° in 2θ, and used in crystallinity determinations according to the method of Ruland[26], as modified by Vonk[37]. A special difficulty arises from the fact that in most of the scattering curves there is no obvious way of separating the crystalline peaks from the background of amorphous scattering. In order to obtain reliable crystallinity values, the shape of the amorphous halo below the various peaks was assumed to correspond to the shape of the halo occurring in the curve obtained from the liquid crystalline material. This was recorded for one sample (4, B-N 3:1) while it was held at ~300°C. In order to make it relevant to samples investigated at room temperature, it was translated to slightly higher angles to correct for the shift due to the thermal expansion of the sample. The magnitude of this translation amounted to 1.3° in 2θ. The result for sample 3 (B-N 3:1), annealed at 251°C is shown in *Figure 10*. Because a degree of arbitrariness is involved in this procedure, the absolute crystallinity values obtained are, as ever, of limited accuracy. However, we believe the actual quoted percentages to be correct to within ±2, and find that the reproducibility is of the order of ±0.5. Furthermore, the degree of crystallinity appears to be largely independent of molecular weight and composition, although it has a tendency to fall with increasing annealing temperature, presumably as the consequence of the broad melting range typical of the random copolymeric material[38], in that the rapid cooling after the heat treatment meant that the component which had melted out was not given full opportunity to reform. The crystallinities measured as a function of composition, molecular weight, and heat treatment, are all in the range of 17.5–25.5% (*Table 2*). The only significant indication of an influence of composition on crystallinity is the value for the 1:1 material, which at 18% (both as-drawn and annealed) is 3–4% below the crystallinities of the polymers of other compositions and broadly similar molecular weights.

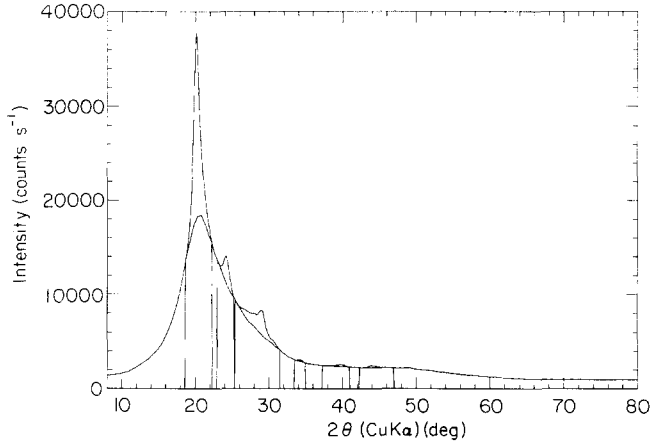

Figure 10 Powder diffraction curve of sample 3 (B-N 3:1), annealed at 251°C, showing the separation of the crystalline peaks from the background of amorphous scattering

DISCUSSION

A significant aspect of this study is the observation, on annealing, of two apparently distinct orthorhombic phases in copoly(HBA–HNA). They have been designated O′ and O″, and are classified according to the different separations of the 1 1 0 and 2 0 0 diffraction peaks (3–4°2θ for the O′ phase compared with ~1°2θ for the O″ before annealing).

The formation of either the O′ or O″ phase depends primarily upon the HBA–HNA ratio. Compositions which are more HBA-rich than 2:1 show the O′ phase, while those which are more HNA-rich show the O″ structure. Both were observed together in the 2:1 polymer. The difference in annealing behaviour of HBA-rich and HNA-rich samples is clearly illustrated in *Figure 11*. The HNA-rich unit cells maintain similar basal

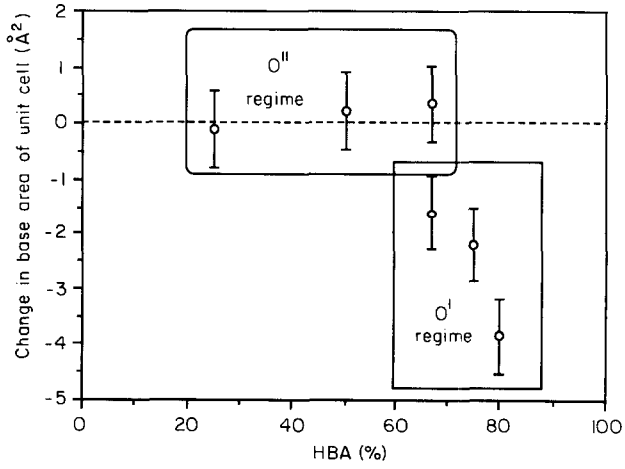

Figure 11 Dependence on copolymer composition of the change in base area of the unit cell (Å²) which accompanies the annealing process. The change is expressed as the cross-sectional area of the unit cells for the highest annealing temperatures minus that of the equivalent PH unit cell

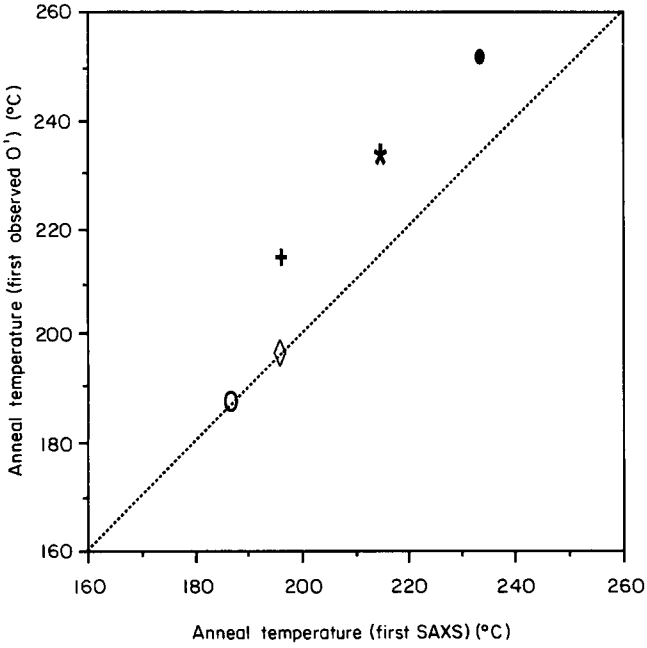

Figure 12 Correlation plot of the anneal temperatures for onset of SAXS with those for occurrence of the PH to O′ phase transformation. The symbols +, ◇, ∗, ● and ○ represent samples 2, 3, 4, 5 and 6, respectively, as described in *Table 1*. The broken line is for $x = y$

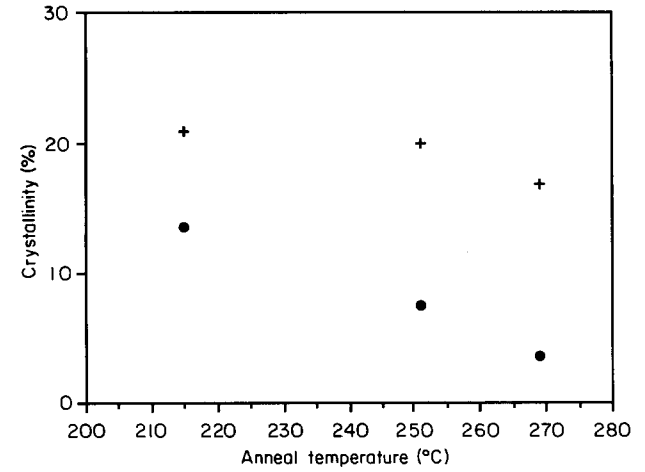

Figure 13 Comparison of the percentage crystallinity which is obtained after quenching an annealed sample (+) with that which is present at the anneal temperature before quenching (●) for specimens of B–N 3:1 (sample 3). Measurements are taken from the powder diffraction curves in *Figure 5*

areas across the range of anneal temperatures, and it is therefore proposed that the gradual increase in the otherwise small 1 1 0/2 0 0 separation in the O″ phase represents a change in shape of the cell base, the a/b ratio moving further away from the value of $\sqrt{3}$ characteristic of the hexagonal cell. However, in HBA-rich copolymers, there is a noticeable reduction in the cross-sectional area of the unit cell during the annealing process as the new O′ phase forms from its PH precursor.

The central observation in this work is the requirement of the formation of the denser O′ phase before discrete SAXS maxima are seen. The correlation is illustrated in *Figure 12*, in which the anneal temperature at which the orthorhombic phase first appeared is plotted against that necessary to induce the discrete small-angle maxima. The implication is that both the PH crystals of the HBA-rich and the O″ phase of the HNA-rich samples have very similar densities to that of the non-crystalline phase. Correspondingly, it must be emphasized again that the absence of small-angle maxima does not imply the absence of crystallites, which can be seen microscopically in all samples. Indeed, the absolute degree of crystallinity measured as a function of composition, molecular weight and heat treatment has been found to be within the range 17.5–25.5%. Furthermore, the crystallinity tends to show, if anything, a modest decrease with increasing anneal temperatures. The only exception is the 4:1 sample, in which a significant increase from 17 to 25.5% was recorded for an anneal at 269°C. The more typical behaviour is demonstrated for sample 3 (3:1) in *Figure 13*, which also illustrates that the crystallinity obtained after quenching from the anneal is considerably greater than that actually present at the anneal temperature.

The combination of measurements of SAXS long periods and the crystallinity provide, on the assumption of a simple two-phase model, a tentative means of estimating the crystal thickness. The results are shown in *Figure 14*. They indicate that the first recordable thickness of 60 Å, corresponding to the first appearance of the SAXS maxima on annealing can be increased to ~120 Å by annealing at higher temperatures, and that this increase is irrespective of the particular mechanism of thickening. However, in the absence of SAXS measurements at the anneal temperature we must urge caution with respect to this interpretation, as an aperiodically arranged component of crystallinity, possibly that formed on cooling from the anneal temperature, may contribute to the measured crystallinity but not affect the SAXS long period. A recent paper from this laboratory[21], which brings microscopy to bear in specifically addressing the thickness issue, concludes that the crystal thickness in samples annealed at ~200°C for 1 h is 73 Å.

CONCLUSIONS

1. In the HBA-rich compositions (2:1 and 3:1) the PH crystal structure formed on quenching from the

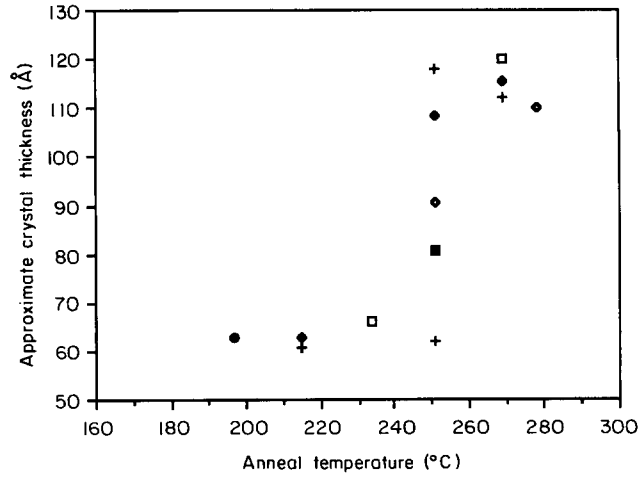

Figure 14 Crystal thicknesses calculated from the SAXS long periods and crystallinity measurements of samples which were quenched to room temperature after annealing for 6 h at the specified temperatures. HBA–HNA ratio/sample number: (□) 4:1/1; (◆) 3:1/2; (+) 3:1/3; (◇) 3:1/4; (■) 3:1/5; (●) 2:1/6

mesophase melt, is joined by an O′ phase on annealing at temperatures within ~80°C of the melting point. The dimensions of this unit cell correspond to those predicted from the weighted average of the two parent homopolymer structures assuming Vegard's law. The 4:1 sample showed the presence of the O′ phase in the unannealed condition.

2. For the two compositions which are closest to the HNA end of the range (1:3 and 1:1) the unit cell is orthorhombic at all temperatures, although the distortion from hexagonal is less than in the case of O′. This structure is known as O″. Annealing leads to an increase in the orthorhombic distortion, although the basal area of the cell appears unchanged. Polymers of 2:1 composition initially show the PH structure but develop the O″ phase as well as O′ on annealing.
3. Discrete small-angle maxima only appear in annealed examples of the HBA-rich polymers. Their appearance correlates well with the development of the O′ phase. The crystallite long period is in the region of 300 Å, in good agreement with corresponding measurements from microscopy. This value increases towards 800 Å in samples annealed above 230°C and there is evidence of a specific doubling mechanism operating in the lower molecular weight samples of 3:1 composition.
4. The absence of discernible SAXS peaks in all the rapidly quenched samples implies that the density of the non-crystalline phase is very close to that of the crystal phase. Such correspondence is consistent with the need for strain minimization at the crystal surfaces normal to the chain direction, for in the absence of chain folding, such strain could otherwise only be avoided through the segregation of chain ends or crystal tilting. The absence of contraction on crystallization is a processing advantage for the material as it contributes to very accurate reproduction of mould detail.
5. Careful measurements of crystallinity from the WAXS traces gives room temperature values in the region of 20% for all quenched samples. The exact values for the 1:1 polymer are slightly lower, at 18%. Annealing leads to a decrease in crystallinity by up to 5% in all samples except 4:1 where the initial decrease is followed by an increase for an anneal at 269°C.

ACKNOWLEDGEMENTS

The authors are indebted to Dr T. Nicholson (Department of Materials Science and Metallurgy) for considerable assistance with computing facilities and software. We would also wish to thank Dr A. R. Faruqi (MRC Laboratory of Molecular Biology) and Dr W. Bras (Daresbury), as well as the Department of Education for Northern Ireland who provided an XNI Studentship Award to support the research.

REFERENCES

1 Golombok, R., Hanna, S. and Windle, A. H. *Mol. Cryst. Liq. Cryst.* 1988, **155**, 281
2 Hanna, S. *PhD Thesis* University of Cambridge, 1988
3 Lemmon, T. J., Hanna, S. and Windle, A. H. *Polym. Commun.* 1989, **30**, 1
4 Donald, A. M. and Windle, A. H. *J. Mater. Sci. Lett.* 1985, **4**, 58
5 Spontak, R. J. and Windle, A. H. *J. Mater. Sci.* 1990, **25**, 2727
6 Cheng, S. Z. D., Janimak, J. J., Zhang, A. and Zhou, Z. *Macromolecules* 1989, **22**, 4240
7 Kaito, A., Kyotani, M. and Nakayama, K. *Macromolecules* 1990, **23**, 1035
8 Hanna, S., Lemmon, T. J. and Windle, A. H. 'Polymer Science: Contemporary Themes' (Ed. S. Sivaram), Tata McGraw-Hill, New Delhi, 1991
9 Sun, Z., Cheng, H. M. and Blackwell, J. *Macromolecules* 1991, **24**, 4162
10 Hoffman, J. D., Frolen, L. J., Ross, G. S. and Lauritzen Jr, J. I. *J. Res. Natl Bur. Stand.* 1975, **79A**, 671
11 Dlugosz, J., Fraser, G. V., Grubb, D., Keller, A., Odell, J. A. and Goggin, P. L. *Polymer* 1976, **17**, 471
12 Grubb, D. T. and Keller, A. *J. Polym. Sci., Polym. Phys. Edn* 1980, **18**, 207
13 Schultz, J. M., Fischer, E. W., Schaumburg, O. and Zachmann, H. G. *J. Polym. Sci., Polym. Phys. Edn* 1980, **18**, 239
14 Barham, P. J. and Keller, A. *J. Polym. Sci., Polym. Phys. Edn* 1989, **27**, 1029
15 Vonk, C. G. *J. Polym. Sci., Polym. Phys. Edn* 1990, **28**, 1871
16 Dreyfuss, P. and Keller, A. *J. Macromol. Sci. Phys.* 1970, **B4**, 811
17 Windle, A. H. *J. Mater. Sci.* 1975, **10**, 1959
18 Grubb, D. T., Prasad, K. and Adams, W. *Polymer* 1991, **32**, 1167
19 Baltá Calleja, F. J., Santa Cruz, C., Chen, D. and Zachmann, H. G. *Polymer* 1991, **32**, 2252
20 Viney, C. and Windle, A. H. *Mol. Cryst. Liq. Cryst.* 1985, **129**, 75
21 Hanna, S., Lemmon, T. J., Spontak, R. J. and Windle, A. H. *Polymer* 1992, **33**, 3
22 Blundell, D. J. *Polymer* 1982, **23**, 359
23 Butzbach, G. D., Wendorff, J. H. and Zimmermann, H. J. *Makromol. Chem., Rapid Commun.* 1985, **6**, 821
24 Hanna, S. and Windle, A. H. *Polymer* 1988, **29**, 236
25 Hanna, S. and Windle, A. H. *Polymer* 1992, **33**, 13
26 Ruland, W. *Acta Cryst.* 1961, **14**, 1180
27 Vonk, C. G. and Pipjers, A. P. *J. Appl. Cryst.* 1981, **14**, 8
28 Blackwell, J., Leiser, G. and Gutierrez, G. A. *Macromolecules* 1983, **16**, 1418
29 Mitchell, G. R. and Windle, A. H. *Colloid Polym. Sci.* 1985, **263**, 230
30 Chivers, R. A., Blackwell, J. and Gutierrez, G. A. *Polymer* 1984, **25**, 435
31 Lieser, G. *J. Polym. Sci., Polym. Phys. Edn* 1983, **21**, 1611
32 Kricheldorf, H. R. and Schwarz, G. *Makromol. Chem.* 1983, **184**, 475
33 Golombok, R. *PhD Thesis* University of Cambridge, 1990
34 Spontak, R. J. and Windle, A. H. *Polymer* 1990, **31**, 1395
35 Spontak, R. J. and Windle, A. H. *J. Polym. Sci., Polym. Phys. Edn* 1992, **30**, 61
36 Lemmon, T. J. *PhD Thesis* University of Cambridge, 1989
37 Vonk, C. G. *J. Appl. Cryst.* 1973, **6**, 148
38 Windle, A. H., Viney, C., Golombok, R., Donald, A. M. and Mitchell, G. R. *Faraday Disc. Chem. Soc.* 1985, **79**, 55